

# A Slab of Liquid Helium-4 with Two Free Surfaces

C.D.H. Williams and A.F.G. Wyatt

*School of Physics, University of Exeter, Exeter EX4 4QL, United Kingdom*

*We describe a method of creating a freely suspended ‘slab’ of superfluid helium-II by using a dense array of  $51\ \mu\text{m}$  diameter parallel cylindrical holes in a glass disc of  $190\ \mu\text{m}$  thickness. By adjusting the chemical potential in the cell, the holes could be made to fill with liquid, and the surface-curvature controlled. We have measured the transmission of atom beams, generated by a thin-film heater and detected with a sensitive bolometer, through this slab at low temperature. The results show that  $R^+$  rotons can undergo total internal reflection at the free liquid surfaces and confirm that the dominant transmission channel is atom- $R^+$  roton-atom with a maximum probability  $p \sim 0.15$  for 5 K atoms.*

*PACS numbers: 67.40.-w 68.03.-g 68.03.Fg 68.03.Cd.*

## 1. INTRODUCTION

Superfluid  $^4\text{He}$  (helium-II) has a unique combination of properties<sup>1</sup> that give rise to the phenomena known as *quantum evaporation*<sup>2-5</sup> and *quantum condensation*<sup>6,7</sup>. These processes occur at the liquid-vacuum free surface and have been investigated experimentally at low temperatures;  $T < 100\ \text{mK}$  is required to suppress scattering by atoms in the vapour and/or thermal excitations. Experiments at Exeter<sup>4,5,7</sup> created excitations in the liquid helium by pulsing a thin-film gold heater. The excitations travelled ballistically to the surface, and there caused evaporation of atoms which, in turn, travelled ballistically through the vacuum before condensing onto a superconducting-transition bolometer operated in constant temperature mode<sup>8</sup>. The measurements of time-resolved atom-flux signals for a variety of heater powers, angles of incidence, and detector positions showed that a single high-energy phonon, an  $R^+$  roton, or an  $R^-$  roton can evaporate a single atom in one-to-one processes that obey the following kinematic rules.

An excitation in the liquid, with wave-vector  $\mathbf{q}$  at angle of incidence  $\theta$

to the surface, can evaporate a single atom, with wave-vector  $\mathbf{k}$  at angle  $\phi$ , subject to the boundary conditions

$$E(q) - E_b = \frac{\hbar^2 k^2}{2m} \quad \text{and} \quad q \sin(\theta) = k \sin(\phi) \quad (1, 2)$$

where  $E(q)$  is the  $^4\text{He}$  excitation spectrum and  $E_b/k_B = 7.15$  K is the binding energy of an atom, mass  $m$ , to the liquid surface at  $T = 0$  K. The experiments put upper-bounds on the size of any other quasiparticles involved in the evaporation<sup>9</sup>, and only processes in which a single excitation was annihilated ejecting a single atom were observed. Experiments<sup>6,7</sup> have also shown that the reverse process, quantum condensation, creates high-energy phonons and  $R^+$  rotons in the same manner.

The possibility of quantum evaporation was proposed several decades ago<sup>10</sup>, and the kinematic rules that govern it are well-established. However, measurements of the probabilities associated with these processes are problematic. In essence, this is because the zinc superconducting-transition detectors used in the experiments detect rotons with an unknown, and very small, responsivity. In principle, a way to overcome this difficulty would be to suspend a ‘slab’ of helium, with two parallel free surfaces, in a vacuum. The experiment would condense an atom beam onto one surface creating excitations that propagate across the slab and evaporate atoms from the other surface. Such an experiment only requires relative measurements of the incident and emitted atom fluxes, so the absolute responsivity of the detector does not need to be known; the parallel slab appears simply to attenuate the flux of atoms. A limitation of the method is that it gives the product of the condensation and evaporation probabilities; an advantage of the method is that it is direct and easy to interpret. A less detailed report of some of the measurements made using this method has been published elsewhere<sup>11</sup>.

## 2. THE EXPERIMENT

In principle<sup>12</sup>, it is possible to prepare a slab with flat surfaces by using a cesium barrier to isolate the slab and its helium reservoir from the other parts of the experiment. Our attempts to do this were thwarted because the cesium needed to be melted *in situ* in order to prepare a clean surface. Although the vapour pressure of cesium is very low, it was sufficient to contaminate the glass holes supporting the slab with a very thin layer of cesium. The cesiated surfaces were not wetted by helium and, as a result, it proved impossible to control the amount of helium forming the slab reliably.

To avoid having to use cesium we modified the experiment and exploited capillary action. To form and control the ‘slab’ (Fig. 1) we used a thin glass

## A Slab of Liquid $^4\text{He}$ with Two Free Surfaces

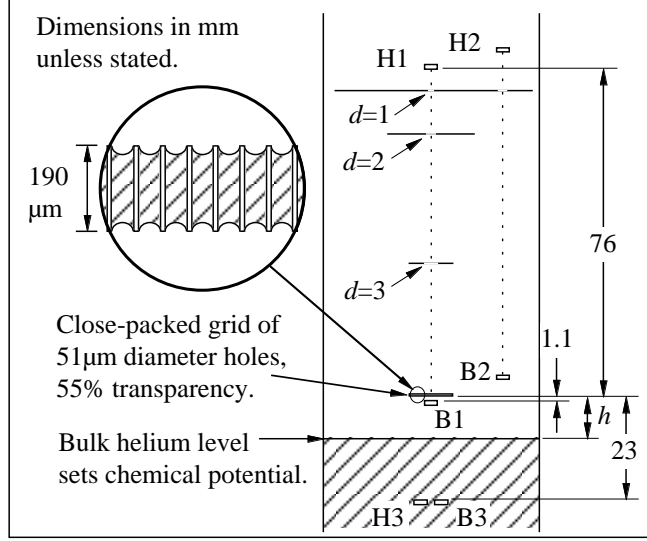


Fig. 1. Schematic diagram of the grid and the cell. The paths of the atom beams are shown by dotted lines.

plate with a set of parallel holes perpendicular to the plate (Collimated Holes Inc., California, 95008 USA). The holes were cylindrical with length  $l = 190 \mu\text{m}$  and diameter  $d = 51 \pm 1 \mu\text{m}$ .

The Helmholtz free energy, at  $T = 0 \text{ K}$ , of the liquid in the pore at height  $h$  above the free surface of the bulk reservoir is

$$F = F_0 + \sigma A + \rho g h V \quad (3)$$

where  $F_0$  includes the van der Waals interaction with the substrate and is essentially a constant in this situation,  $A$  and  $V$  are respectively the free surface area and volume of the liquid in the pore,  $\sigma = 3.75 \times 10^{-4} \text{ J m}^{-2}$  is the surface free energy<sup>13</sup>, and  $\rho = 145 \text{ kg m}^{-3}$  is the density.

We used Maple<sup>14</sup> to calculate the free energy of the configurations shown in Fig. 2. We found that the pore is unconditionally ‘empty’ when  $h \geq 4\sigma/\rho g d = 20.7 \text{ mm}$ , *i.e.* there is a thin Rollin film coating the pore. As the level of the reservoir is raised,  $h$  decreases and the Rollin film thickness increases but the pore remains essentially empty. The chemical potential in the film is equal to that of the reservoir. At  $h = 2\sigma/\rho g d = 10.3 \text{ mm}$ , this state is unstable to any fluctuations and the pore fills with liquid. Equilibrium requires that the top and bottom free surfaces form concave spherical caps with radii of curvature  $R = 2\sigma/\rho g h$ . As  $h$  is further decreased, the pore remains closed and  $R$  increases. If  $h$  is increased starting from  $h < 10.3 \text{ mm}$  then  $R$  increases to maintain equilibrium until  $R = d/2$ , at  $h = 20.7 \text{ mm}$ ,

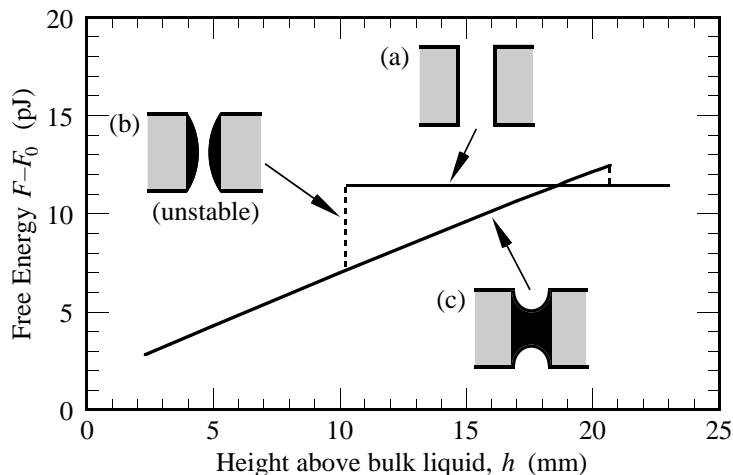


Fig. 2. Free energy minima for three configurations of helium in a pore (see text) at height  $h$  above bulk liquid. (a) The pore is ‘empty’, but coated with superfluid film; (b) the pore is ‘closing’; (c) the pore is ‘closed’, the helium has concave spherical caps at both ends.

at which point the energy barrier preventing the hemispherical caps moving towards each other, and then touching, vanishes so the liquid drains out of the pore leaving it empty. The behaviour is hysteretic because there is an energy barrier separating the empty and closed states when  $10.3 \text{ mm} < h < 20.7 \text{ mm}$ . We have estimated this barrier by assuming that the helium in the pore fluctuates into a surface of revolution given in terms of cylindrical co-ordinates concentric with the pore by

$$r = \frac{d \cosh(2\lambda z/l)}{2 \cosh(\lambda)} \quad (4)$$

where the parameter  $\lambda \geq 0$  sets the volume of liquid. This is a computationally convenient function and, for a given  $h$ , the corresponding minimum energy is close to ( $< 0.33 \text{ pJ}$  greater than) that of a closed pore. We find energy barriers of  $\sim 1 \text{ pJ}$ , which are much larger than thermal fluctuations; the pores are effectively bistable and a mechanical disturbance is needed to induce a transition between the empty and closed states.

The capillary tube, through which the helium was added to the cell, was above the grid and the pores were closed when the reservoir level was at  $h = 19.2 \text{ mm}$ . The minimum value of  $h$  we used was  $2.3 \text{ mm}$  so the maximum value of  $R$  was  $2.29 \times 10^{-4} \text{ m}$ , which is  $4.50d$ . Under these conditions the maximum angle between the liquid surface and the horizontal occurred at the rim of the pore and was  $6.4^\circ$ .

### A Slab of Liquid $^4\text{He}$ with Two Free Surfaces

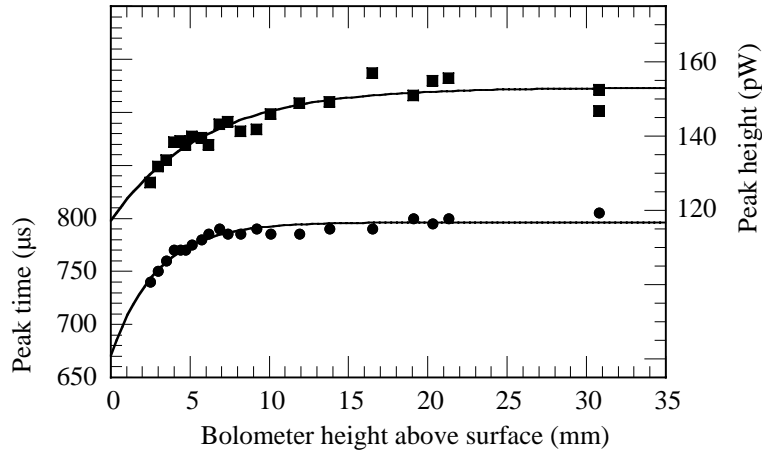


Fig. 3. The dependence of the peak height (squares) and arrival time (circles) in the H2–B2 reference signal on the height of B2 above the bulk liquid level. This example is for a  $1.0\ \mu\text{s}$   $0.5\ \text{mW}$  pulse.

The curvature of the free surface of liquid in the pores was controlled by changing the height of helium in the cell. We were able to measure the height of the bulk liquid surface to within  $0.1\ \text{mm}$  using sonar; a heater–bolometer pair (H3–B3), was positioned  $22.5\ \text{mm}$  below the glass plate. The heater sent a  $0.1\ \mu\text{s}$   $20\ \text{mW}$  pulse of ultrasound, velocity  $238.3\ \text{m s}^{-1}$ , to the free surface where it was reflected back to the bolometer.

The atom beam was created by a  $5\ \mu\text{s}$   $2.0\ \text{mW}$  electrical pulse applied to a  $1 \times 1\ \text{mm}$  thin-film gold heater (H1) covered by the superfluid film. The cell was maintained at  $\sim 60\ \text{mK}$  by a dilution refrigerator; at this temperature the vapour pressure is negligible and an atom beam is not scattered by ambient atoms. Three laser-aligned collimators in front of the heater formed the  $5\ \text{mm}$  diameter beam of atoms incident on the glass capillary array. The angular width of the useful beam was  $\pm 0.8^\circ$ . The geometry was chosen to ensure that the atoms travelled essentially parallel to the axis of the experiment and perpendicular to the plate. A  $1\ \text{mm}^2$  superconducting zinc-film bolometer (B1) was positioned  $1.1\ \text{mm}$  below the plate. It was biased with a magnetic field to reduce its transition temperature and linearised by employing a constant temperature mode of operation<sup>8</sup>.

Another heater–bolometer pair (H2–B2), but without the intervening capillary array, was included to monitor the influence of changing  $h$  on the detector due to changes in the thickness of the helium film covering it (Fig. 3). The intrinsic time constant of the detectors was  $\sim 1\ \mu\text{s}$ , but this does not include the time needed to equilibrate the heat deposited by atoms condensing onto the helium film adjacent to the bolometer. The energy flux

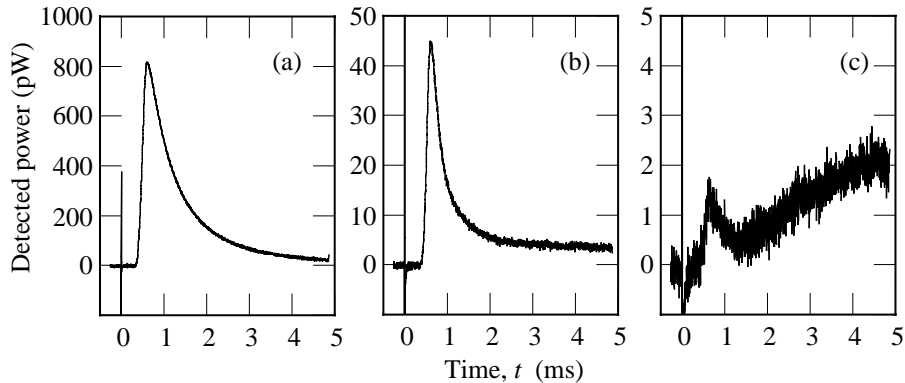


Fig. 4. Typical (B1) signals taken at various stages of the experiment: (a) empty pores, (b) liquid-filled pores,  $h = 2.3$  mm (minimum surface curvature), (c)  $h = 19$  mm.

detected by the bolometer is interpreted as the atom energy flux convolved with a time constant of  $\sim 100 \mu\text{s}$  arising from this mechanism, and this causes a delay of  $\sim 50 \mu\text{s}$  in the peak of the recorded signal.

The empty-pore atom signal (Fig. 4a) was recorded with the liquid level 28 mm below the pores. The level was then raised in steps by adding isotopically pure helium<sup>15</sup> to the cell. It can be seen, Fig. 4c, that filling the pores with helium attenuated the signal by between two and three orders of magnitude. We attribute the rising baseline in this figure to riplons, created by atoms condensing onto the collimators, arriving at the bolometer. Reducing the curvature of the surface, by decreasing  $h$ , increased the signal (Fig. 4b). Figure 5 summarises the results and shows the peak height of the detected atom pulses measured at different values of  $h$ .

### 3. DISCUSSION

*A priori*, a condensing atom may create riplons, phonons, an  $R^+$  roton, an  $R^-$  roton, or some combination of these excitations<sup>7</sup>. However, the large magnitude and the characteristic  $h$  dependence of the measured transmission (Fig. 5) both identify the dominant transmission process as being due to  $R^+$  rotons. We have confirmed this with a computer program that uses the kinematic rules (equations 1 and 2 above) to model the the atom–roton–atom trajectories from the incident beam to the detector.

The model assumes a parallel and uniform beam of atoms incident on the top free surface of the liquid in the pores. Each atom creates an  $R^+$  roton which will travel at some angle to the pore axis until it hits either the

### A Slab of Liquid $^4\text{He}$ with Two Free Surfaces

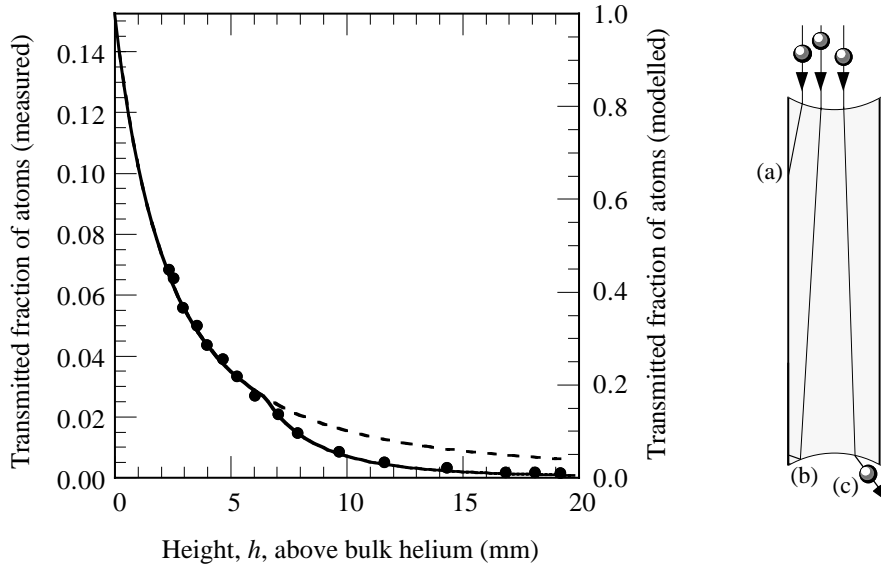


Fig. 5. Fraction of transmitted atoms (points) compared with model (solid line) using  $R^+$  roton wave vector  $22\text{ nm}^{-1}$  and assuming that  $p_{+a}p_{a+} = 1$ . The effect of omitting total internal reflection from the model is also shown (dashed line). The diagram illustrates the model used to interpret the experiment and shows typical events for  $h = 10\text{ mm}$  (a)  $R^+$  scatters at solid surface and is lost, (b) total internal reflection of  $R^+$  at free surface, (c) atom transmitted.

lower free surface or the pore wall, in which case it is assumed to be lost. The roton evaporates an atom if it hits the lower surface and the angle of incidence on the lower free surface is less than the critical angle for total internal reflection (TIR). For our geometry and a 4.5 K atom, for example, this is possible for  $h > 6.5\text{ mm}$ . If TIR occurs, then the roton is treated as lost. The result of this model is shown as the solid line in Fig. 5 with the scale on the right-hand side; the dashed line omits the TIR process from the model. The data agrees with the solid line. The model results must be scaled by a constant factor  $p_{a+}p_{+a}$ , where  $p_{a+}$  is product of the probability of an atom creating an  $R^+$  roton and  $p_{+a}$  is the probability of an  $R^+$  roton evaporating an atom, to match the measured transmitted fractions.

The results of this analysis, for atoms of 4.5 K energy, are the curves in Fig. 5. The points on the figure have been corrected, using the H2-B2 measurements, for the changing bolometer responsivity with  $h$  (Fig. 3). There is agreement between the measurements and the model provided atoms creating rotons outside the critical angle for TIR are treated as untransmitted. The onset of total internal reflection at  $h = 6.5\text{ mm}$  is clearly apparent in

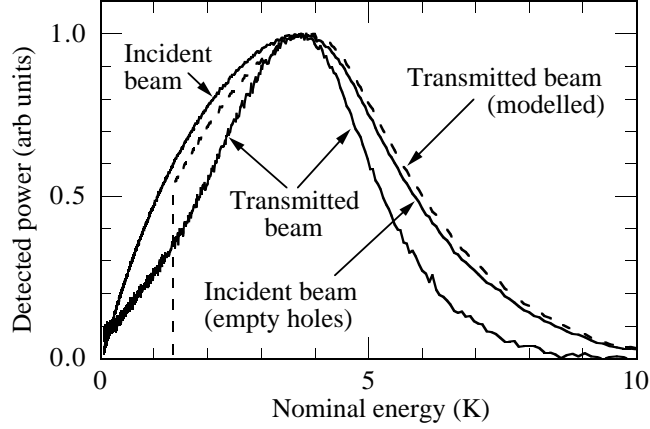


Fig. 6. Signals from Fig. 4 (a) and (b) rescaled to show the dependence on nominal atom energy  $E = 0.5m_{\text{He}}(D/t)^2$  where  $D$  is the heater–detector distance and  $t$  is the signal arrival-time.

both the measurements and the model; this feature is unique to  $R^+$  rotons and confirms our identification of the transmission mechanism. The ratio of the atom flux extrapolated to  $h = 0$  to the atom flux through the empty pores is 0.15 *i.e.*  $p_{a+}p_{+a} = 0.15$  for an atom energy 4.5 K. This result is not significantly affected by the atom energy selected to analyse the results, providing it is in the range 4–5 K. If, instead of the peak heights, we use integrals of the signals over the range  $200 \mu\text{s}$  to  $983 \mu\text{s}$  (this is the time for atoms of energy 1.44 K, which is the minimum required to create a roton, to travel 76 mm) the ratio is 0.12.

Figure 6 shows the measured atom fluxes through closed pores, with  $h = 2.3 \text{ mm}$ , and empty pores as functions of nominal atom energy calculated from time of flight. The presence of the liquid helium attenuates the signal by a factor of 14.8 at the peak. It might be expected that there should be no signal for atom energies less than 1.4 K when there is helium filling the pores, because such atoms do not have enough energy to create rotons; the energy of the roton minimum is 8.6 K and this must be greater than the sum of the condensation energy, 7.16 K, and the kinetic energy. However, the detector time-constant in our experiment means that the ‘low energy’ signal cannot be identified with a unique atom energy; there is a contribution from higher energy atoms that arrived earlier. There is, however, a significant change in slope around 1.4 K which can be seen in the figure. From the modelling we find the peak atom energy that best fits our data is  $\sim 4.5 \text{ K}$ . The position of the peak in Fig. 6 is at 3.7 K but the shift to this lower value is accounted for by the detector time-constant, as described above.

## A Slab of Liquid $^4\text{He}$ with Two Free Surfaces

Previous experiments have shown that for a roton, the probability of quantum evaporation does not depend strongly on angle of incidence or energy<sup>4,9</sup>. There is some indirect evidence that the evaporation probability for  $R^+$  rotons is around 0.35<sup>16,17</sup> and increases with energy<sup>18</sup>. It is likely that other processes occur besides the one-to-one processes. For example, an atom incident on the surface may create multiple ripples<sup>19,20</sup>. It seems that the simultaneous creation of a free atom and a ripplon has a low probability as there is no angular spreading of the phonon-evaporated atom beam due to the co-creation of low-energy ripples<sup>9</sup>. However, Fig. 6 suggests that the transmission probability decreases with increasing atom energy, and this is consistent with the expectation that the probability of ripplon production increases with the energy of the condensing atom energy<sup>21</sup>.

The transmission of helium atoms through a thin slab of helium-II has been treated in recent theoretical calculations<sup>22–24</sup>. Some of these<sup>23,24</sup> have included the possibility of creating ripples. They find that the ‘transmission’ probability is typically  $\sim 0.1$  over much of the energy range above  $\sim 10.5$  K, although low-energy excitations (7.2–9.5 K) have higher probability,  $\sim 0.25$ , and there is a deep minimum at 10 K, which corresponds to the position of the roton minimum in their model, where the rotons have zero group-velocity. Dalfovo *et al.*<sup>25</sup> predicted that  $p_{+a} = p_{a+}$  and we note that if we take  $p_{+a} = 0.35 \pm 0.03$ <sup>16</sup> then our average value implies that  $p_{a+} \sim 0.34$ . The measured value of transmission is of similar magnitude to the theoretical values calculated by Campbell *et al.*<sup>23</sup>.

## 4. CONCLUSIONS

We have shown that it is possible to prepare a ‘slab’ of superfluid with two free surfaces and to investigate its properties experimentally. Not surprisingly, we found that the curvature of the free surface of helium-II in this system is accurately described by conventional thermodynamics. We have used this system to show that the transmission across the liquid slab is mediated by  $R^+$  rotons; these are created by quantum condensation at the top surface and they quantum evaporate atoms at the bottom surface. The average transmission probabilities are remarkably high,  $p_{+a}p_{a+} = 0.12 \pm 0.01$ , as can be appreciated by noting that  $\sqrt{0.12} = 0.35$ . The experiment also demonstrates a number of other interesting properties of  $R^+$  rotons:  $R^+$  rotons of energy  $\sim 12$  K can propagate without appreciable attenuation through 0.2 mm of liquid  $^4\text{He}$  at low temperature;  $R^+$  rotons undergo total internal reflection when  $q \sin(\theta) = k$  at the free surface of liquid helium, and also that  $R^+$  rotons do not scatter elastically from a glass surface, pre-

C.D.H. Williams and A.F.G. Wyatt

sumably because they scatter diffusely and maybe mode-change.

## ACKNOWLEDGEMENTS

It is a pleasure to acknowledge M.A.H. Tucker for his help in designing and making parts of the apparatus, helpful discussions with E. Krotscheck, L. Pitaevskii, and E.P.S.R.C for financial support.

## REFERENCES

1. D. R. Tilley and J. Tilley, *Superfluidity and Superconductivity*, 3rd ed. (Inst. of Physics, Bristol, 1990).
2. M. J. Baird, F. R. Hope, and A. F. G. Wyatt, *Nature* **304**, 325 (1983).
3. F. R. Hope, M. J. Baird, and A. F. G. Wyatt, *Phys. Rev. Lett.* **52**, 1528 (1984).
4. M. Brown and A. F. G. Wyatt, *J. Phys. Condens. Matter* **2**, 5025 (1990).
5. M. A. H. Tucker and A. F. G. Wyatt, *J. Low Temp. Phys.* **113**, 615 (1998).
6. M. Brown and A. F. G. Wyatt, in *Proc. Phonons 89* (World Scientific, Singapore, 1990), p. 1050.
7. M. Brown and A. F. G. Wyatt, *J. Phys. Condens. Matter* **15**, 4717 (2003).
8. C. D. H. Williams, *Meas. Sci. Technol.* **1**, 322 (1990).
9. C. D. H. Williams, *J. Low Temp. Phys.* **113**, 11 (1998).
10. P. W. Anderson, *Phys. Lett.* **29A**, 563 (1969).
11. C. D. H. Williams and A. F. G. Wyatt, *Phys. Rev. Lett.* **98**, art. 085301 (2003).
12. A. F. G. Wyatt, talk at IVth Workshop on Quantum Fluid Clusters, Shloss Ringberg, Bavaria. (unpublished).
13. C. Vicente, W. Yao, H. J. Maris, and G. M. Seidel, *Phys. Rev. B* **66**, art. 214504 (2002).
14. K. Heal, M. Hansen, and K. Rickard, *Maple V: Learning Guide* (Springer-Verlag, New York, 1998).
15. P. C. Hendry and P. V. E. McClintock, *Cryogenics* **27**, 131 (1987).
16. P. Fozooni, D. S. Spencer, and M. Lea, *Japan J. Appl. Phys.* **26** **S26-3**, 281 (1987).
17. C. Enss *et al.*, *Physica B* **194-196 part 1**, 515 (1994).
18. C. D. H. Williams, *J. Low Temp. Phys.* **113**, 627 (1998).
19. D. O. Edwards, G. G. Ihas, and C. P. Tam, *Phys. Rev. B* **16**, 3122 (1977).
20. A. F. G. Wyatt, M. A. H. Tucker, and R. F. Cregan, *Phys. Rev. Lett.* **74**, 5236 (1995).
21. P. Echenique and J. Pendry, *J. Phys. C: Solid St. Phys* **9**, 3183 (1976).
22. A. K. Setty, J. W. Halley, and C. E. Campbell, *Phys. Rev. Lett.* **79**, 3930 (1997).
23. C. E. Campbell, E. Krotscheck, and M. Saarela, *Phys. Rev. Lett.* **80**, 2169 (1998).
24. C. E. Campbell, E. Krotscheck, and M. Saarela, *J. Low Temp. Phys.* **113**, 519 (1998).
25. F. Dalfovo, L. Pitaevskii, and S. Stringari, *Czech J. Phys.* **46**, 391 (1996).